Generating quantum nonlocal entanglement with mechanical rotations

Marko Toroš,[1] Maria Chiara Braidotti,[2] Swain Ashutosh,[2] Mauro Paternostro,[3,4] Miles Padgett,[2] and Daniele Faccio[2]

[1]*Faculty of Mathematics and Physics, University of Ljubljana, Jadranska 19, SI-1000 Ljubljana, Slovenia*

[2]*School of Physics and Astronomy, University of Glasgow, Glasgow G12 8QQ, United Kingdom*

[3]*Università degli Studi di Palermo, Dipartimento di Fisica e Chimica—Emilio Segrè, via Archirafi 36, I-90123 Palermo, Italy*

[4]*Centre for Theoretical Atomic, Molecular, and Optical Physics, School of Mathematics and Physics, Queen's University, Belfast BT7 1NN, United Kingdom*

(Received 26 July 2024; accepted 31 July 2025; published 27 August 2025)

Recent experiments have searched for evidence of the impact of noninertial motion on the entanglement of particles. The success of these endeavors has been hindered by the fact that such tests were performed within spatial scales that were only "local" when compared to the spatial scales over which the noninertial motion was taking place. We propose a Sagnac-like interferometer that, by challenging such bottlenecks, is able to achieve entangled states through a mechanism induced by the mechanical rotation of a photonic interferometer. The resulting states violate the Bell-Clauser-Horne-Shimony-Holt (Bell-CHSH) inequality all the way up to the Tsirelson bound, thus signaling strong quantum nonlocality. Furthermore, we show that *the Bell-CHSH* inequality remains violated even without using any form of postselection up to the value $1+\sqrt{2}$. Our results demonstrate that mechanical rotation can be thought of as resource for controlling quantum nonlocality with implications also for recent proposals for experiments that can probe the quantum nature of curved spacetimes and noninertial motion.

DOI: 10.1103/84vr-nnvs

I. INTRODUCTION

The seminal work of J. S. Bell allowed to infer the inherent incompatibility of quantum mechanics with the (classically acceptable) assumption of local realism posed by Einstein, Podolsky, and Rosen [1,2]. The falsification of a Bell inequality, which would be fully satisfied by any local realistic theory, has been reported in countless experiments [3–11], and recognized with the 2022 Nobel Prize in Physics.

Independently, questions about relativity led Sagnac to establish a now widespread method for measuring rotational motion using optical interferometry [12,13]. Two counterpropagating signals acquire a phase difference proportional to the angular frequency of rotation [14–17]. This insight led to the development of the ring laser [18] and fiber-optical gyroscopes [19,20], with the current state of the art achieving sub-shot-noise sensitivities [21]. The Sagnac effect has been shown to induce interference at the level of quantum systems, with experimental implementations in matter-wave interferometry [17] and single-photon platforms [22].

More recently, photonic technologies have enabled the exploration of rotation-induced quantum phenomena with two-photon experiments. Polarization-entangled photon pairs were shown to be robust against a $30 \times g$ acceleration achieved on a rotating centrifuge [23]. Using a Hong-Ou-Mandel interferometer on a rotating platform, it was found that low-frequency mechanical rotations affect bunching statistics [24]. Super resolution and Sagnac phase sensitivity beyond the shot-noise limit was achieved in Ref. [25] using path-entangled NOON states, and milliradian phase resolution was achieved in Ref. [26], allowing the measurement of the Earth's angular frequency of $\sim 10\,\mu$Hz. Furthermore, it was suggested that photonic entanglement can be revealed or concealed using noninertial motion accessible to current experiments [27]. Using a Hong-Ou-Mandel interferometer with nested arms, it was demonstrated that photonic behavior can change from bunching to antibunching (i.e., from bosonic to fermionic) solely due to mechanical rotations [28]. Moreover, it was shown that rotational motion can change the phase of polarization entangled states enabling transitioning between pairs of Bell states [29]. Crucially, these experiments involve quantum states that are entangled prior to rotation and rotation is only used to modify, probe, or enhance existing quantum features.

A significant conceptual step further is to demonstrate the actual generation of entanglement using noninertial motion. The approach proposed in Ref. [30] made use of a multipath Sagnac interferometer to achieve a maximally entangled path-polarization state of a single photon. Such state would be suitable for quantum noncontextuality tests aimed at ascertaining whether observables can be assigned preexisting values prior to measurements [31]. In principle, the generated entanglement could also be transferred to two spatially separated physical systems [32], but the experimental demonstration of such procedures remains experimentally challenging [33,34]. It is thus not immediately obvious whether the single-photon scheme proposed in Ref. [30] would allow to unambiguously demonstrate the genera-

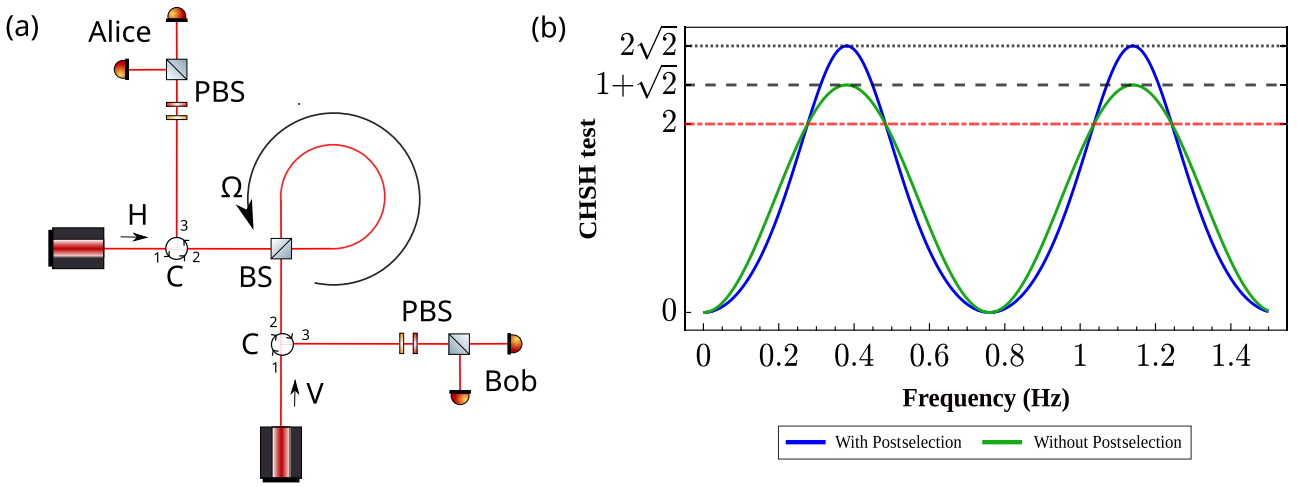

FIG. 1. (a) Photonic setting for the rotation-controlled generation of quantum nonlocal states of polarization. Two photons are initially prepared in the separable state $|HV\rangle$ and injected into the setup. The circulators, denoted by C, first send the photons into a Sagnac loop, and then redirect them toward two individual detection stages (only the directional paths, 1 to 2 and 2 to 3, are allowed by the circulators). As the photons entering the Sagnac loop through BS are initially prepared in orthogonal polarization states, they do not interact at any point via electromagnetic couplings. We measure the polarization of the photons with a standard Bell detection scheme. (b) Theoretical prediction of the violation of the Bell-CHSH inequality. *With Postselection* refers to the case where one photon is measured using the setup at the top (managed by Alice) and one photon is measured with the setup on the right (managed by Bob). *Without Postselection* refers to the case where all the photons are considered in the analysis, which includes the detection of one photon by Alice and one photon by Bob as well as of both photons by either Alice or Bob. For concreteness, we have set the photon wavelength to $\lambda = 1\,\mu\text{m}$ ($\omega = 2\pi c/\lambda$) and the interferometric area to $\sim 7.8\,\text{m}^2$ (e.g., 10 loops of fiber with radius $r = 0.5\,\text{m}$ with a total length of $\sim 31.5\,\text{m}$). We predict that a violation ($|S| > 2$) occurs periodically with the rotation frequency as stated by Eq. (13). The maximum violation is first achieved for $\Omega_{\text{Bell}} \sim 0.4\,\text{Hz}$, and the condition $|S| > 2$ is achieved in the interval $\Omega \in 0.4 \pm 0.1\,\text{Hz}$ (see Appendix A for more details).

tion of genuine quantum (nonlocal) entanglement as opposed to local entanglement.

In a different context, recent theoretical studies in quantum gravity [35,36] have proposed schemes where the generation of two-particle nonlocal entanglement can be used to witness the quantumness of the gravitational interaction mediator. These proposals fit within a more general framework of studies where researchers pursue methodologies to test the quantumness or nonclassicality of the involved parties [37], regardless of the type of interaction (see also results in optomechanics and biophotonics [38,39]).

Inspired by these two-party schemes, in this work, we propose an experimentally viable scheme—fully accessible to current photonic technology—in which rotation itself is the mechanism that generates nonlocal entanglement between two initially unentangled photons. This marks a shift, from manipulating the entanglement to demonstrating its rotationally induced creation. Our scheme consists of a single Sagnac fiber loop, linear optics elements, photon-pair sources, and a Bell-test detection setup, all placed on a rotating platform. We find that an initially separable two-photon state can be transformed into a maximally entangled state of polarization that violates significantly the Bell-Clauser-Horne-Shimony-Holt (Bell-CHSH) inequality [40] as a function of the angular frequency of rotation, obtaining a simple formula for the frequency required to saturate Tsirelson's bound [41]. Furthermore, we show that even *without any form of postselection*, the Bell-CHSH inequality remains violated for the same angular frequencies of rotation, achieving the maximum value $1 + \sqrt{2}$ [42]. We conclude by briefly discussing the interpretation of the uncovered link between mechanical motion and quantum nonlocality.

II. PROPOSED SCHEME

We consider the configuration shown in Fig. 1(a), where two single photons are propagating through the system. The full setup involves a pulsed laser source (not shown), pumping two spatially separated type-I nonlinear crystals, each producing photon pairs via spontaneous parametric down-conversion (SPDC). One photon from each pair is detected to herald the presence of its twin, resulting in two heralded single photons that are mutually uncorrelated, as they originate from independent SPDC processes. These signals are first directed into a Sagnac loop through circulators and a beam splitter (BS), and then toward two spatially separated Bell-detection apparatuses. We assume that two independent photons are initially prepared in the separable state:

$$|\psi_{\text{i}}\rangle = \hat{a}_H^\dagger \hat{b}_V^\dagger |0\rangle \equiv |H\,V\rangle, \tag{1}$$

where $\hat{a}_H$ ($\hat{b}_V$) denotes horizontal H (vertical V) polarization mode.

As the two photons enter the Sagnac loop through BS, the state changes according to a beam-splitter transformation into

$$|\psi_{\text{i}}\rangle \to |\psi_1\rangle = \tfrac{1}{2}(\hat{a}_H^\dagger + i\hat{b}_H^\dagger)(i\hat{a}_V^\dagger + \hat{b}_V^\dagger)|0\rangle, \tag{2}$$

where $\hat{a}$ ($\hat{b}$) denoteS the corotating (counter-rotating) mode. The effect of mechanical rotation is to introduce Sagnac phases with a sign depending on the sense of motion of the

particular mode [27]. From Eq. (2), we thus find

$$|\psi_1\rangle \to |\psi_2\rangle = \frac{1}{2}\left[e^{i\frac{\phi}{2}}\hat{a}_H^\dagger + ie^{-i\frac{\phi}{2}}\hat{b}_H^\dagger\right]\left[ie^{i\frac{\phi}{2}}\hat{a}_V^\dagger + e^{-i\frac{\phi}{2}}\hat{b}_V^\dagger\right]|0\rangle, \quad (3)$$

where the phase factors have been introduced to account for the relative phase acquired by the counterpropagating modes. Irrespective of the medium, shape of the interferometer or the location of the center of rotation, the Sagnac phase is given by [14]

$$\phi = \frac{4A\omega\Omega}{c^2}, \quad (4)$$

where A is the interferometer area, c is the speed of light in vacuum, $\omega = 2\pi c/\lambda$ is the angular frequency of the photons (λ is the photon wavelength), $\Omega = 2\pi f$, and f is the mechanical frequency of the rotating platform. Moreover, any phase affecting differently the two polarizations would simply factor out of Eq. (3). Similarly, if there is some random noise affecting the corotating path, then the same noise will also affect the counter-rotating path, again factoring out of Eq. (3). Hence, classical phase delays arising through experimental imperfections will not change the final result. To generate differential phases depending on the direction of rotation, the only plausible mechanism is the Sagnac effect.

As the photons exit the central loop through the BS, we apply the inverse beam-splitter transformation to Eq. (3), giving us

$$\begin{aligned}|\psi_2\rangle \to |\psi_{\rm tot}\rangle &= \frac{1}{4}[(e^{i\phi/2}(-i\hat{a}_H^\dagger + \hat{b}_H^\dagger) + ie^{-i\phi/2}(\hat{a}_H^\dagger - i\hat{b}_H^\dagger) \\ &\times (ie^{i\phi/2}(-i\hat{a}_V^\dagger + \hat{b}_V^\dagger) + e^{-i\phi/2}(\hat{a}_V^\dagger - i\hat{b}_V^\dagger)]|0\rangle. \quad (5)\end{aligned}$$

After rearranging the terms in Eq. (5), we find

$$|\psi_{\rm tot}\rangle = \frac{1}{2}\sqrt{3+\cos(2\phi)}|\psi_{\rm fav}\rangle + \frac{\sin\phi}{\sqrt{2}}|\psi_{\rm unfav}\rangle, \quad (6)$$

where we have introduced the normalized states

$$|\psi_{\rm fav}\rangle = \left[\frac{(\cos\phi - 1)\hat{a}_H^\dagger\hat{b}_V^\dagger}{\sqrt{3+\cos(2\phi)}} + \frac{(\cos\phi + 1)\hat{b}_H^\dagger\hat{a}_V^\dagger}{\sqrt{3+\cos(2\phi)}}\right]|0\rangle, \quad (7)$$

$$|\psi_{\rm unfav}\rangle = \frac{1}{\sqrt{2}}[\hat{a}_H^\dagger\hat{a}_V^\dagger - \hat{b}_H^\dagger\hat{b}_V^\dagger]|0\rangle. \quad (8)$$

$|\psi_{\rm fav}\rangle$ represents the case when each pair of detectors detects one photon, i.e., Alice detects mode a and Bob detects mode b or vice versa, while $|\psi_{\rm unfav}\rangle$ represents the case when both photons arrive at the same pair of detectors, i.e., either both to Alice or both to Bob. As we want to compute quantum correlations between Alice and Bob we will refer to $|\psi_{\rm fav}\rangle$ and $|\psi_{\rm unfav}\rangle$ as the *favorable* and *unfavorable* state, respectively.

III. VIOLATION OF THE BELL-CHSH INEQUALITY

To quantify the degree of generated nonlocality we can compute the Bell-CHSH function S [40]

$$S = E(\boldsymbol{a},\boldsymbol{b}) - E(\boldsymbol{a},\boldsymbol{b}') + E(\boldsymbol{a}',\boldsymbol{b}) + E(\boldsymbol{a}',\boldsymbol{b}'), \quad (9)$$

where the quantum correlations are given by

$$E(\boldsymbol{v},\boldsymbol{u}) = \langle\psi|\hat{A}_{\boldsymbol{v}}\hat{B}_{\boldsymbol{u}}|\psi\rangle, \quad (10)$$

$|\psi\rangle$ is the state of the system, and $\hat{A}_{\boldsymbol{v}}$ and $\hat{B}_{\boldsymbol{u}}$ correspond to the measurements performed by Alice and Bob, respectively ($\boldsymbol{v} = \boldsymbol{a}, \boldsymbol{a}'$ and $\boldsymbol{u} = \boldsymbol{b}, \boldsymbol{b}'$ denote unit vectors parametrizing the measurement operators). The four terms appearing in Eq. (9) are associated with four different joint measurements performed by Alice and Bob. Local realism enforces the Bell-CHSH inequality $|S| \leqslant 2$. However, as we will see, suitable choices of the angular frequency of rotation, encoded in the phase ϕ in Eq. (6), allow to violate such constraint. We show below that the Bell-CHSH inequality is violated up to the value $|S| = 1+\sqrt{2}$ by considering the total state in Eq. (6), establishing the phenomena of rotationally induced quantum nonlocality (Sec. III A). Furthermore, we show that Tsirelson's bound $|S| = 2\sqrt{2}$ can be achieved by postselecting coincidences at the detectors (Sec. III B).

A. Nonlocality without postselection

We define the observables $\hat{A}_{\boldsymbol{u}}$ and $\hat{B}_{\boldsymbol{v}}$ by prescribing how they act on the basis states of our Hilbert space (we recall that observables, which are linear maps, can always be defined in this way). The total Hilbert space, and in particular its basis, can be read out from the total final state $|\psi_{\rm tot}\rangle$ in Eqs. (6)–(8). On the Hilbert subspace spanned by $\hat{a}_H^\dagger\hat{b}_V^\dagger|0\rangle$ and $\hat{b}_H^\dagger\hat{a}_V^\dagger|0\rangle$ (i.e., the basis states of the favorable subspace), we define $\hat{A}_{\boldsymbol{a}} \equiv \boldsymbol{a}\cdot\boldsymbol{\sigma}$ and $\hat{B}_{\boldsymbol{b}} \equiv \boldsymbol{b}\cdot\boldsymbol{\sigma}$, where $\boldsymbol{\sigma} = (\sigma_x, \sigma_y, \sigma_z)$ is the vector of the Pauli matrices. In order to achieve the highest violation of the Bell test, we choose the vectors $\boldsymbol{a} = (1,0,0)$, $\boldsymbol{a}' = (0,1,0)$, $\boldsymbol{b} = (1,1,0)/\sqrt{2}$, and $\boldsymbol{b}' = (-1,1,0)/\sqrt{2}$. On the Hilbert subspace spanned by $\hat{a}_H^\dagger\hat{a}_V^\dagger|0\rangle$ and $\hat{b}_H^\dagger\hat{b}_V^\dagger|0\rangle$ (i.e., the basis states of the unfavorable subspace), we define $\hat{A}_{\boldsymbol{a}} = \mathbb{I}$ and $\hat{B}_{\boldsymbol{a}} = \mathbb{I}$, where $\mathbb{I}$ denotes the identity operator [42].

To compute the Bell-CHSH value, we consider the total state without any postselection; i.e., we set $|\psi\rangle \equiv |\psi_{\rm tot}\rangle$. Inserting Eq. (6) into Eq. (9), we eventually find

$$S = \left(1+\sqrt{2}\right)\sin^2(\phi). \quad (11)$$

In particular, by setting $\phi = \pi/2 + k\pi$ ($k \in \mathcal{Z}$), the state in Eq. (6) reduces to $|\psi_{\rm tot}\rangle = \frac{1}{\sqrt{2}}(|\psi_{\rm fav}\rangle + |\psi_{\rm unfav}\rangle)$, i.e.,

$$|\psi_{\rm tot}\rangle = \tfrac{1}{2}[-\hat{a}_H^\dagger\hat{b}_V^\dagger + \hat{b}_H^\dagger\hat{a}_V^\dagger + \hat{a}_H^\dagger\hat{a}_V^\dagger - \hat{b}_H^\dagger\hat{b}_V^\dagger]|0\rangle, \quad (12)$$

and we achieve the maximum violation $|S| = 1+\sqrt{2}$. This occurs when the mechanical frequency Ω takes the values

$$\Omega_{\rm Bell} \equiv \frac{\pi c^2}{8A\omega}(2k+1), \quad (k \in \mathcal{Z}). \quad (13)$$

Here, $k < 0$ ($k > 0$) would correspond to an (anti)clockwise sense of rotation.

The experimentally measurable Bell-CHSH correlation will be obtained by repeating the experiment with a large number of initial photon pairs in order to gather enough statistics. In Fig. 1(b), we plot the Bell-CHSH function for a set of values of the relevant physical parameters that are well within reach of existing photonic technology with previous experiments already achieving the required sensitivities [23–29].

Importantly, the Bell-CHSH violation depends critically only on the mechanical rotation. We recall that two initial states in Eq. (1) consist of photons that are in orthogonal polarization modes, and hence do not interact at the beam splitter or

via any electromagnetic interaction, and that no postselection has been performed on the total final state in Eq. (6). The results captured by Eq. (9) thus depend critically only on the angular frequency of rotation Ω: by tuning its value we can generate quantum nonlocality, while without mechanical rotation no quantum nonlocality can be established.

B. Tsirelson's bound with postselection

We now consider the state conditional on the postselection of the events that provide coincidences at the detectors, i.e., quantum correlations between Alice and Bob, where we disregard the events arising from the unfavorable state $|\psi_{\text{unfav}}\rangle$ in Eq. (8). We discuss the probability of coincidence detection in Appendix B, which remains greater than 50%, and hence does not pose a severe limitation. We can rewrite the remaining favorable state $|\psi_{\text{fav}}\rangle$ defined in Eq. (7) as

$$|\psi_{\text{fav}}\rangle = \frac{\cos(\phi)+1}{\sqrt{3+\cos(2\phi)}}|H\,V\rangle + \frac{\cos(\phi)-1}{\sqrt{3+\cos(2\phi)}}|V\,H\rangle, \quad (14)$$

where we have introduced the commonly used notation $\hat{a}_H^\dagger \hat{b}_V^\dagger|0\rangle \equiv |H\,V\rangle$ and $\hat{a}_V^\dagger \hat{b}_H^\dagger|0\rangle \equiv |V\,H\rangle$.

We first note that for $\phi = 0$ (corresponding to the case without mechanical rotation) we always remain in the initial state $|H\,V\rangle$, which is separable. More generally, we note that for $\phi = \pi\,k$ ($k \in \mathcal{Z}$) we either remain in the initial state $|H\,V\rangle$ (k even) or transform into the flipped polarization state $|V\,H\rangle$ (k odd). However, for any other value of ϕ we find that Eq. (14) will be in an entangled state. In particular, for $\phi = \pi/2 + \pi\,k$ ($k \in \mathcal{Z}$) Eq. (14) transforms into the maximally entangled Bell state

$$|\psi_{\text{fav}}\rangle = \tfrac{1}{\sqrt{2}}(|H\,V\rangle - |V\,H\rangle), \quad (15)$$

which is usually denoted as the $|\Psi^-\rangle$ state.

To compute the Bell-CHSH value, we set $|\psi\rangle \equiv |\psi_{\text{f}}\rangle$ in Eq. (9) to obtain the value

$$S = 4\sqrt{2}\frac{\sin^2(\phi)}{3+\cos(2\phi)}. \quad (16)$$

In particular, as stated in Eq. (15), by setting $\phi = \pi/2 + k\pi$ ($k \in \mathcal{Z}$), the state in Eq. (14) reduces to the Bell state $|\Psi^-\rangle$ and we achieve the notorious Tsirelson's bound $|S| = 2\sqrt{2}$ [41]. In Fig. 1(b), we plot the Bell-CHSH function defined in Eq. (16) for the same set of values as for the case without postselection to ease the comparison.

Saturating Tsirelson's bound depends critically on two steps: (1) on the postselection step from Eq. (6) to (14), where we have discarded the unfavorable state, and (2) on a nonzero rotationally induced phase $\phi \neq 0$, which arises only for nonzero frequencies of rotation $\Omega \neq 0$. The postselection step is, however, not enough to induce entanglement in the absence of mechanical rotation as discussed above for the case $\phi = 0$. Furthermore, even without any form postselection we have shown that the Bell-CHSH inequality remains violated (see Sec. III A).

IV. DISCUSSION

We have proposed a method for the controlled generation of quantum nonlocality using mechanical rotation that achieves the map

$$\hat{a}_H^\dagger \hat{b}_V^\dagger|0\rangle \to \tfrac{1}{2}[(\cos\phi - 1)\hat{a}_H^\dagger \hat{b}_V^\dagger + (\cos\phi + 1)\hat{b}_H^\dagger \hat{a}_V^\dagger + \sin\phi\,(\hat{a}_H^\dagger \hat{a}_V^\dagger - \hat{b}_H^\dagger \hat{b}_V^\dagger)]|0\rangle. \quad (17)$$

The minimalist derivation is fully contained in Eqs. (1)–(8), assuming only the Sagnac phase and the form of the beamsplitter transformation. By controlling the angular frequency of the mechanical rotation, Ω, and hence the corresponding Sagnac phase, $\phi \equiv \phi(\Omega)$, we have shown that we can prepare either separable or nonlocally entangled final states.

The map in Eq. (17) satisfies a number of desiderata: (1) For $\phi = 0$, the transformation reduces to the identity map, i.e., $\mathcal{M} = \mathbb{I}$. In other words, without mechanical rotation, the state remains invariant (and classical). (2) For $\phi = \pi\,k$ ($k \in \mathbb{Z}$), the transformation in Eq. (17) is either the identity operation (even k) or induces a polarization flip (odd k). The latter case shows that mechanical rotation can be used to swap the polarization state of photon pairs. (3) For $\phi = (2k+1)\pi/2$ ($k \in \mathbb{Z}$), we obtain the state in Eq. (12), which is predicted to violate the Bell-CHSH inequality. The first line of Eq. (17) (corresponding to Alice and Bob detecting each one photon) reduces to the Bell state $|\Psi^-\rangle$, which is expected to induce a maximal violation of the Bell-CHSH inequality given by the Tsirelson's bound [41]. However, even in absence of any form of postselection, the total final state in Eq. (17) produces a violation of the Bell-CHSH inequality up to the value $S = 1 + \sqrt{2}$ [42].

The scheme is also robust against imperfections and noise due to the inherent protection characteristic of the Sagnac loop. Suppose some unwanted phases would be accumulating depending on the polarization H, V; this would contribute only to a global phase in Eq. (3), but no measurable differential phase would be generated. Similarly, any other random phase affecting the corotating path will automatically affect also the counter-rotating path, thus factoring out without affecting the final state. As shown in Fig. 1(b), the experimental parameters required to test the maximum violation of the Bell-CHSH inequality can be achieved with current photonic technologies by adaptation of previous experimental schemes [23–29]. As such, we do not expect any fundamental or technical issue in the implementation of this proposal (see Appendix C for the analysis of background noise, dark counts, and detector inefficiencies).

A further benefit of the proposed scheme is also that it does not rely on specific models, but rather on the well-established Bell-CHSH test. The violation arises only when we tune the mechanical frequency of rotation to the interval centered on the value Ω_{Bell}. Hence, nonzero mechanical rotation is a critical factor for generating nonlocality in this setup; i.e., we can legitimately speak of *rotationally induced nonlocality*.

The question of how to interpret the experiment is of course nonetheless interesting. In this work, we have provided a simple yet very effective and powerful theoretical interpretation only relying on the Sagnac phase. While here we have not shown this, the Sagnac phase is of intrinsic relativistic origin. Evidence of such nature stems from Eq. (4), which depends on the speed of light in vacuum and not on that of photons in a medium, suggesting that its origin is related to the spacetime metric (we refer the interested reader to the reviews [14–17]).

However, more formal interpretations within quantum theory in curved space [27], broader quantum field theoretic framework [43], or a general relativistic context [44–47] are also possible. The possibility to further such thoughts and interpret the spacetime metric as in a superposition, along the lines of Ref. [30], thus reaching out to the domain of quantum reference [48,49] frames, will be the topic of further investigations.

ACKNOWLEDGMENTS

M.T. acknowledges funding from the Slovenian Research and Innovation Agency (ARIS) under Contracts No. N1-0392, No. P1-0416, and No. SN-ZRD/22-27/0510 (RSUL Toroš) and from the Leverhulme Trust (RPG-2020-197). M.C.B. acknowledges support from the UK EPSRC (EP/Y008308/1). M.P. acknowledges the support by the Horizon Europe EIC Pathfinder project QuCoM (Grant Agreement No. 101046973), the Leverhulme Trust Research Project Grant UltraQuTe (Grant No. RGP-2018-266), the Royal Society Wolfson Fellowship (RSWF/R3/183013), the UK EPSRC (EP/T028424/1), and the Department for the Economy Northern Ireland under the US-Ireland R&D Partnership Program. D.F. acknowledges support from the Royal Academy of Engineering and the UK EPSRC (EP/W007444/1).

APPENDIX A: ANGULAR VELOCITY FLUCTUATIONS

The presented scheme is robust with respect to angular velocity fluctuations, $\delta\Omega$, of the rotating platform. For example, let us focus on the region of the first peak shown in Fig. 1, where $\phi \in [0, \pi]$. We can then readily estimate the minimum (maximum) angular frequency Ω_- (Ω_+) at the boundaries of the interval, where we have a violation of the Bell inequality, i.e., determined by the condition $|S| > 2$. We define the maximum allowed angular velocity fluctuations as $\delta\Omega \equiv \Omega_+ - \Omega_{\rm Bell}$ (or equivalently $\delta\Omega = \Omega_{\rm Bell} - \Omega_-$ given the the symmetric shape of the peak), such that for angular frequencies in the interval

$$\Omega \in \Omega_{\rm Bell} \pm \delta\Omega, \tag{A1}$$

we have a violation of the Bell inequality. From Eqs. (4) and (11) [or from Eqs. (4) and (16)], we find that the maximum allowed angular velocity fluctuations are given by

$$\delta\Omega = \frac{c^2}{4A\omega} \arctan\sqrt{\frac{\sqrt{2}-1}{2}}. \tag{A2}$$

In particular, for the parameters listed in Fig. 1 we find the value $\delta\Omega = 2\pi \times 0.1$Hz, which does not pose a challenging requirement for the rotation control of low-frequency rotating platforms [24,28]. A similar analysis on the sensitivity of the Bell-CHSH violation can be performed also for the other peaks at higher ($k > 0$) or negative ($k < 0$) values of $\Omega_{\rm Bell}$.

APPENDIX B: COINCIDENCE DETECTION

The detection method considered here relies on four-photon coincidences: Two photon pairs are generated by two different SPDC processes. One photon from each pair is heralded [not shown in Fig. 1(a)], ensuring that the other photon propagates within the system. In this frame, the loss of one photon does not affect the measurement; it will only result in longer acquisition times. In the following discussion, we do not explicitly include the heralding process; all references to two-photon detection or coincidence events are made under the implicit assumption that the corresponding heralded photons have been successfully detected.

A further point needs to be made: in the case with postselection, not all two-photons detections produce an increase in the number of counts; only when the top-left pair of detectors (Alice) detects one photon and the bottom-right pair of detectors (Bob) detects one photon we are able to update the experimental value of S defined in Eq. (16) [see Fig. 1(a)]—we need a coincidence measurement between Alice and Bob. We can find the resulting reduction in the number of counts by noting that the numerical prefactors of Eqs. (6) and (7) give the associated probability amplitudes. Hence, squaring and summing the amplitudes of the terms $\propto \hat{a}^\dagger \hat{b}^\dagger$ we find the probability of detection $(\cos^2(\phi) + 1)/2$, which gives a 50% reduction in the statistics at $\Omega = \Omega_{\rm Bell}$. The case without postselection is unaffected by this reduction in the probability of detection as all the photons are taken into account.

APPENDIX C: EFFECT OF NOISE ON BELL-CHSH TEST

Noise in the form of background noise, dark counts, and detector inefficiencies can significantly affect the quantum correlations relevant to the Bell-CHSH test. In this section, we quantitatively examine the effect of such noise on the Bell-CHSH test and consequently on the extent of violation of local realism. Such investigations are of paramount importance when trying to assess the feasibility of our scheme for experimental implementation. One possible noise source is a passive coupling mechanism caused by backscattering from the cavity mirrors, in particular the BS surfaces in our setup. While such coupling could, in principle, lead to spurious mode interactions or background contributions, it is not expected to play a significant role in our case. The single photons do not populate a well-defined intracavity mode, and therefore do not establish conditions for mode locking through mirror-induced feedback. Furthermore, due to the low generation efficiencies, as well as the finite spectral bandwidth of the photons, their coherence length remains short. This prevents significant temporal or spatial overlap between corotating and counter-rotating photon wave packets, effectively suppressing coherent interference effects arising from backscattering.

Low pair-generation efficiencies also play a crucial role in suppressing unwanted multipair emission events, which can introduce noise into the measurement outcomes. Similar to what occurs in static (nonrotating) measurements, such multipair events contribute to a small but nonnegligible background. However, their impact can be minimized by operating at low pump powers, reducing the probability of higher-order emissions.

A separate treatment is necessary when considering a noise model in which the subsystems associated with Alice and Bob are subject to independent error processes with noise error probability ϵ_A and ϵ_B, respectively [50]. To simplify the presentation and estimate the magnitude of the effects, we here assume that the noise error probability of Alice's subsystem, ϵ_A, is the same as Bob's, ϵ_B ($\epsilon_A = \epsilon_B = \epsilon$), and that

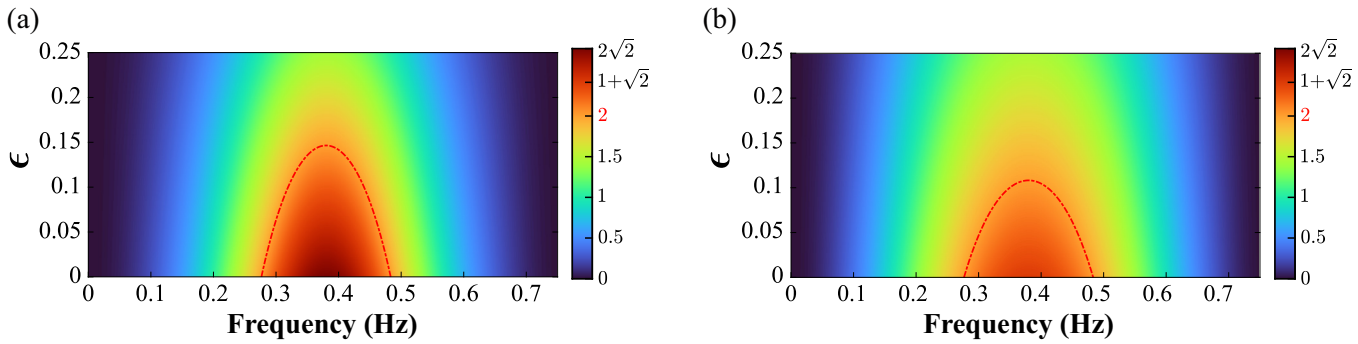

FIG. 2. Variation of the Bell-CHSH parameter S with frequency and error probability ϵ. (a) Case with postselection. (b) Case without postselection. We use same values for wavelength λ and interferometric area as used in Fig. 1.

$0 < \epsilon \ll 1$. Hence, we can write the total system statistical operator $\hat{\rho}$ as

$$\hat{\rho} = (1-2\epsilon)\hat{\rho}_{AB} + \epsilon\left(\hat{\rho}_A \otimes \tfrac{1}{2}\right) + \epsilon\left(\tfrac{1}{2} \otimes \hat{\rho}_B\right), \tag{C1}$$

where $\hat{\rho}_{AB} = |\psi_3\rangle\langle\psi_3|$, with $|\psi_3\rangle$ the interferometer output state given by Eq. (6), while $\hat{\rho}_A = \mathrm{tr}_B(|\psi_3\rangle\langle\psi_3|)$ and $\hat{\rho}_B = \mathrm{tr}_A(|\psi_3\rangle\langle\psi_3|)$ are the reduced states of Alice's and Bob's subsystem. We use $\hat{\rho}$ to compute the Bell-CHSH function S from Eq. (9) for two cases: without postselection (Sec. III A) and with postselection (Sec. III B).

To evaluate E(a, b) in S, we use

$$E(\boldsymbol{a}, \boldsymbol{b}) = \mathrm{tr}(\hat{O}\,\hat{\rho}), \tag{C2}$$

where $\hat{O}$ is equal to $(\boldsymbol{a}\cdot\boldsymbol{\sigma}) \otimes (\boldsymbol{b}\cdot\boldsymbol{\sigma})$ for the case with postselection (we have one photon for each subsystem). However, for the case without postselection, we use the approach suggested in Ref. [42]: Here, $\hat{O}$ is equal to $(\boldsymbol{a}\cdot\boldsymbol{\sigma}) \otimes (\boldsymbol{b}\cdot\boldsymbol{\sigma})$ when each subsystem receives one photon, while $\hat{O}$ is equal to identity for the other cases when Alice or Bob's subsystem receive more than one photon each.

Using this formalism, for the case with postselection, we get

$$S = (1-2\epsilon)4\sqrt{2}\frac{\sin^2\phi}{3+\cos 2\phi}. \tag{C3}$$

Similarly for the case without postselection, we get

$$S = (1-2\epsilon)(1+\sqrt{2})\sin^2\phi + \epsilon\sin^2\phi. \tag{C4}$$

The variation of S with frequency and the error probability ϵ is shown in Fig. 2. As expected, for the case with postselection, we see a violation of the Bell-CHSH inequality for a higher error probability compared to the case without postselection. Nevertheless, it is worth noticing that the Bell-CHSH parameter can exceed the threshold value $S = 2$ in both cases. This is due to the fact that S measures the nonlocality of the state and hence that our final state is indeed nonlocal, even if not maximally entangled.

[1] J. S. Bell, On the Einstein Podolsky Rosen paradox, Phys. Phys. Fiz. **1**, 195 (1964).

[2] A. Einstein, B. Podolsky, and N. Rosen, Can quantum-mechanical description of physical reality be considered complete? Phys. Rev. **47**, 777 (1935).

[3] S. J. Freedman and J. F. Clauser, Experimental test of local hidden-variable theories, Phys. Rev. Lett. **28**, 938 (1972).

[4] A. Aspect, P. Grangier, and G. Roger, Experimental tests of realistic local theories via Bell's theorem, Phys. Rev. Lett. **47**, 460 (1981).

[5] A. Aspect, J. Dalibard, and G. Roger, Experimental test of Bell's inequalities using time-varying analyzers, Phys. Rev. Lett. **49**, 1804 (1982).

[6] G. Weihs, T. Jennewein, C. Simon, H. Weinfurter, and A. Zeilinger, Violation of Bell's inequality under strict Einstein locality conditions, Phys. Rev. Lett. **81**, 5039 (1998).

[7] J.-W. Pan, D. Bouwmeester, M. Daniell, H. Weinfurter, and A. Zeilinger, Experimental test of quantum nonlocality in three-photon Greenberger–Horne–Zeilinger entanglement, Nature (London) **403**, 515 (2000).

[8] M. A. Rowe, D. Kielpinski, V. Meyer, C. A. Sackett, W. M. Itano, C. Monroe, and D. J. Wineland, Experimental violation of a Bell's inequality with efficient detection, Nature (London) **409**, 791 (2001).

[9] J.-W. Pan, Z.-B. Chen, C.-Y. Lu, H. Weinfurter, A. Zeilinger, and M. Żukowski, Multiphoton entanglement and interferometry, Rev. Mod. Phys. **84**, 777 (2012).

[10] M. Genovese, Research on hidden variable theories: A review of recent progresses, Phys. Rep. **413**, 319 (2005).

[11] N. Brunner, D. Cavalcanti, S. Pironio, V. Scarani, and S. Wehner, Bell nonlocality, Rev. Mod. Phys. **86**, 419 (2014).

[12] G. M. M. Sagnac, Sur la preuve de la réalité de l'éther lumineux par l'expérience de l'interférographe tournant, C.R. Acad. Sci. **157**, 1410 (1913).

[13] G. Sagnac, L'éther lumineux démontré, C. R. Hebd. Seances Acad. Sci. **157**, 708 (1913).

[14] E. J. Post, Sagnac effect, Rev. Mod. Phys. **39**, 475 (1967).

[15] R. Anderson, H. R. Bilger, and G. E. Stedman, Sagnac effect: A century of Earth-rotated interferometers, Am. J. Phys. **62**, 975 (1994).

[16] G. B. Malykin, The Sagnac effect: Correct and incorrect explanations, Phys. Usp. **43**, 1229 (2000).

[17] B. Barrett, R. Geiger, I. Dutta, M. Meunier, B. Canuel, A. Gauguet, P. Bouyer, and A. Landragin, The Sagnac effect:

20 years of development in matter-wave interferometry, C. R. Phys. **15**, 875 (2014).
[18] W. M. Macek and D. T. M. Davis, Rotation rate sensing with traveling-wave ring lasers, Appl. Phys. Lett. **2**, 67 (1963).
[19] V. Vali and R. W. Shorthill, Fiber ring interferometer, Appl. Opt. **15**, 1099 (1976).
[20] H. C. Lefèvre, The fiber-optic gyroscope, a century after Sagnac's experiment: The ultimate rotation-sensing technology? C. R. Phys. **15**, 851 (2014).
[21] A. D. V. Di Virgilio, F. Bajardi, A. Basti, N. Beverini, G. Carelli, D. Ciampini, G. Di Somma, F. Fuso, E. Maccioni, P. Marsili, A. Ortolan, A. Porzio, and D. Vitali, Noise level of a ring laser gyroscope in the femto-rad/s range, Phys. Rev. Lett. **133**, 013601 (2024).
[22] G. Bertocchi, O. Alibart, D. B. Ostrowsky, S. Tanzilli, and P. Baldi, Single-photon Sagnac interferometer, J. Phys. B: At. Mol. Opt. Phys. **39**, 1011 (2006).
[23] M. Fink, A. Rodriguez-Aramendia, J. Handsteiner, A. Ziarkash, F. Steinlechner, T. Scheidl, I. Fuentes, J. Pienaar, T. C. Ralph, and R. Ursin, Experimental test of photonic entanglement in accelerated reference frames, Nat. Commun. **8**, 15304 (2017).
[24] S. Restuccia, M. Toroš, G. M. Gibson, H. Ulbricht, D. Faccio, and M. J. Padgett, Photon bunching in a rotating reference frame, Phys. Rev. Lett. **123**, 110401 (2019).
[25] M. Fink, F. Steinlechner, J. Handsteiner, J. P. Dowling, T. Scheidl, and R. Ursin, Entanglement-enhanced optical gyroscope, New J. Phys. **21**, 053010 (2019).
[26] R. Silvestri, H. Yu, T. Strömberg, C. Hilweg, R. W. Peterson, and P. Walther, Experimental observation of Earth's rotation with quantum entanglement, Sci. Adv. **10**, eado0215 (2024).
[27] M. Toroš, S. Restuccia, G. M. Gibson, M. Cromb, H. Ulbricht, M. Padgett, and D. Faccio, Revealing and concealing entanglement with noninertial motion, Phys. Rev. A **101**, 043837 (2020).
[28] M. Cromb, S. Restuccia, G. M. Gibson, M. Toroš, M. J. Padgett, and D. Faccio, Mechanical rotation modifies the manifestation of photon entanglement, Phys. Rev. Res. **5**, L022005 (2023).
[29] J. A. Bittermann, M. Fink, M. Huber, and R. Ursin, Non-inertial motion dependent entangled Bell-state, arXiv:2401.05186.
[30] M. Toroš, M. Cromb, M. Paternostro, and D. Faccio, Generation of entanglement from mechanical rotation, Phys. Rev. Lett. **129**, 260401 (2022).
[31] S. Kochen and E. Specker, The problem of hidden variables in quantum mechanics, Indiana Univ. Math. J. **17**, 59 (1967).
[32] S. J. van Enk, Single-particle entanglement, Phys. Rev. A **72**, 064306 (2005).
[33] S. Adhikari, A. S. Majumdar, D. Home, and A. K. Pan, Swapping path-spin intraparticle entanglement onto spin-spin interparticle entanglement, Europhys. Lett. **89**, 10005 (2010).
[34] A. Kumari, A. Ghosh, M. L. Bera, and A. K. Pan, Swapping intraphoton entanglement to interphoton entanglement using linear optical devices, Phys. Rev. A **99**, 032118 (2019).
[35] S. Bose, A. Mazumdar, G. W. Morley, H. Ulbricht, M. Toroš, M. Paternostro, A. A. Geraci, P. F. Barker, M. S. Kim, and G. Milburn, Spin entanglement witness for quantum gravity, Phys. Rev. Lett. **119**, 240401 (2017).
[36] C. Marletto and V. Vedral, Gravitationally induced entanglement between two massive particles is sufficient evidence of quantum effects in gravity, Phys. Rev. Lett. **119**, 240402 (2017).
[37] E. Polino, B. Polacchi, D. Poderini, I. Agresti, G. Carvacho, F. Sciarrino, A. Di Biagio, C. Rovelli, and M. Christodoulou, Photonic implementation of quantum gravity simulator, Adv. Photonics Nexus **3**, 036011 (2024).
[38] T. Krisnanda, M. Zuppardo, M. Paternostro, and T. Paterek, Revealing nonclassicality of inaccessible objects, Phys. Rev. Lett. **119**, 120402 (2017).
[39] T. Krisnanda, C. Marletto, V. Vedral, M. Paternostro, and T. Paterek, Probing quantum features of photosynthetic organisms, npj Quantum Inf. **4**, 60 (2018).
[40] J. F. Clauser, M. A. Horne, A. Shimony, and R. A. Holt, Proposed experiment to test local hidden-variable theories, Phys. Rev. Lett. **23**, 880 (1969).
[41] B. S. Cirel'son, Quantum generalizations of Bell's inequality, Lett. Math. Phys. **4**, 93 (1980).
[42] S. Popescu, L. Hardy, and M. Żukowski, Revisiting Bell's theorem for a class of down-conversion experiments, Phys. Rev. A **56**, R4353(R) (1997).
[43] J. I. Korsbakken and J. M. Leinaas, Fulling-Unruh effect in general stationary accelerated frames, Phys. Rev. D **70**, 084016 (2004).
[44] M. Zych, F. Costa, I. Pikovski, T. C. Ralph, and Č. Brukner, General relativistic effects in quantum interference of photons, Class. Quantum Grav. **29**, 224010 (2012).
[45] A. J. Brady and S. Haldar, Frame dragging and the Hong-Ou-Mandel dip: Gravitational effects in multiphoton interference, Phys. Rev. Res. **3**, 023024 (2021).
[46] S. P. Kish and T. C. Ralph, Quantum effects in rotating reference frames, AVS Quantum Sci. **4**, 011401 (2022).
[47] R. Barzel, D. E. Bruschi, A. W. Schell, and C. Lämmerzahl, Observer dependence of photon bunching: The influence of the relativistic redshift on Hong-Ou-Mandel interference, Phys. Rev. D **105**, 105016 (2022).
[48] Y. Aharonov and T. Kaufherr, Quantum frames of reference, Phys. Rev. D **30**, 368 (1984).
[49] F. Giacomini, E. Castro-Ruiz, and Č. Brukner, Relativistic quantum reference frames: The operational meaning of spin, Phys. Rev. Lett. **123**, 090404 (2019).
[50] N. Brunner, N. Gisin, V. Scarani, and C. Simon, Detection loophole in asymmetric Bell experiments, Phys. Rev. Lett. **98**, 220403 (2007).